Interaction of a Tunnel-like Acoustic Disturbance Field with a Normal Shock Wave: Theory and Simulation

Yuchen Liu * and Lian Duan[†] *The Ohio State University, Columbus, OH, 43210*

The interaction of a nominally normal shock wave with a homogeneous field of acoustic waves (shock/acoustics interaction) is studied using direct numerical simulation (DNS) and linear interaction analysis (LIA). The inflow boundary condition for the DNS of shock/acoustics interaction is prescribed using the saved data of a precursor DNS of boundary-layer acoustic radiation. The DNS results are compared with those of LIA that models linear dynamics for making distinctions between linear and nonlinear mechanisms. The results show that the broadband tunnel noise radiated from the the tunnel-wall turbulent boundary layer can be well represented by an acoustic model with an ansatz of slow acoustic waves. With successful calibration of the model parameters against the precursor tunnel DNS, such an acoustic ansatz can successfully reproduce both the frequency-wavenumber spectra and the temporal evolution of the broadband tunnel noise radiated from the tunnel wall. The study of shock/acoustics interaction showed that a good comparison in the turbulent kinetic energy $\overline{u_k' u_k'}/2$ and pressure fluctuation variance $\overline{p'^2}$ behind the shock was achieved between DNS and LIA. The power spectral density (PSD) of post-shock total pressure $p'_{1,2}$ is found to be similar to that of the pre-shock static pressure p'_1 in both near-field and far-field.

Nomenclature

```
M
          Mach number
Ω
          vorticity (1/s)
          specific heat ratio
γ
Re
         Reynolds number
Re_u
          unit Reynolds number (1/m)
          mean static pressure (Pa)
T
          temperature (K)
U
          mean streamwise velocity (m/s)
          streamwise velocity (m/s)
u
          spanwise velocity (m/s)
          wall-normal velocity (m/s)
w
          streamwise direction of the right-handed Cartesian coordinate (m)
x
          spanwise direction of the right-handed Cartesian coordinate (m)
y
          wall-normal or vertical direction of the right-handed Cartesian coordinate (m)
δ
          boundary layer thickness (m)
          density (kg/m<sup>3</sup>)
ρ
          pressure (Pa)
          speed of sound (m/s)
c
k
          wave number (1/m)
          wave number of the most energetic disturbance structures (1/m)
k_0
          frequency (1/s)
          angular frequency (rad/s)
          wavelength (m)
λ
Subscripts
```

^{*}Graduate Research Assistant, Department of Mechanical and Aerospace Engineering, Student Member, AIAA

[†]Associate Professor, Department of Mechanical and Aerospace Engineering, Senior Member, AIAA

- 1 = pre-shock quantities
- 2 = post-shock quantities
- t = total (stagnation) quantities
- x = streamwise direction component
- y = spanwise direction component
- z = wall-normal or verticle direction component

rms = root mean squared variable

Superscripts

- (\cdot) = standard (Reynolds) averaged variable
- $(\cdot)'$ = fluctuations around standard averages

I. Introduction

Understanding the physics of the interaction between a shock wave and a homogeneous field of acoustic waves (shock/acoustics interaction) are of major theoretical and practical importance. From a theoretical point of view, research on shock/acoustics interaction consists of a fundamental study of the dilatational component of compressible turbulence interacting with a shock wave. According to Kovasznay [1], turbulence can be decomposed into vorticity (rotational velocity), acoustic (pressure and irrotational velocity), and entropy (temperature) modes. Given that each of the Kovasznay modes interacts in its own way with the shock front [2-4], a study of the interaction between a shock wave and a field of broadband acoustic waves helps characterize the behaviors of shock/turbulence interaction in the pure dilatational limit and complements existing studies that have vorticity-dominated turbulence in front of the shock wave. From a practical point of view, one of the important engineering applications of shock/acoustics interaction lies in the measurement of facility freestream disturbances using intrusive Pitot probes in supersonic wind tunnels. The freestream disturbance environment in an unheated supersonic wind tunnel ($M_{\infty} \gtrsim 2.5$) with adequate flow conditioning is dominated by acoustic waves radiated from turbulent boundary layers on tunnel side-walls as illustrated in Figure 1a [5–7], and the Pitot probes are commonly applied for characterizing wind-tunnel freestream disturbances given their ruggedness and their ability to yield data with higher frequencies than the hot-wire anemometers [8–12] (Figure 1b). Given that Pitot probes record the time variation of total (Pitot) pressure behind the probe shock wave (Figure 1c), a study of shock/acoustics interaction is critical to the reconstruction of the incident acoustic disturbances from the post-shock Pitot pressure.

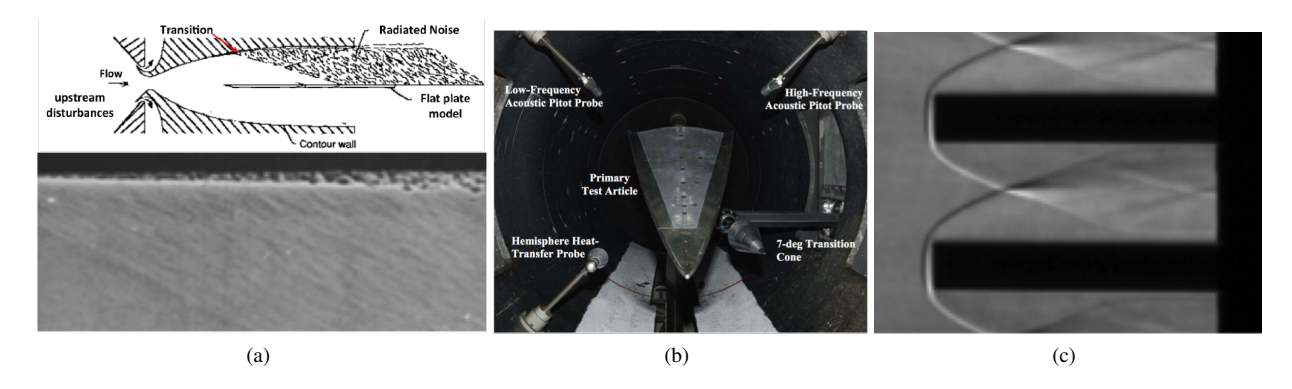


Fig. 1 (a) Sketch of the test core of a Mach 3.5 wind tunnel and experimental image of a shadowgraph for acoustic radiation from the tunnel-wall turbulent boundary layer (adapted from Beckwith and Miller [13]); (b) Example of intrusive Pitot probes mounted in the free stream of a supersonic wind tunnel for freestream-noise measurement (adapted from Bounitch et al. [8]); (c) Schlieren image for freestream Pitot probes and their leading-edge shock in a supersonic wind tunnel (adapted from Masutti et al. [9]).

The interaction of a shock wave with a field of general unsteady disturbances including acoustic waves is amenable to theoretical analysis such as the linear interaction analysis (LIA) [2, 3, 14–18] and the rapid distortion theory (RDT) [19–21]. LIA, which assumes small disturbances and negligible viscous effect, is less restrictive than RDT

and has in general better agreement with experiments. LIA is centered on a mathematical description of a linear two-dimensional (2-D) plane wave interacting with a normal shock wave, and a collection of upstream disturbances can be viewed as a superposition of 2-D plane waves (Fourier modes) over a prescribed spectrum. Although LIA has been widely used for studying the interaction of a shock wave with a spectrum of incident vorticity or entropy waves, there are much fewer LIA for the interaction of a shock wave with a spectrum of incident acoustic waves. The few studies include those by Mahesh et al. [15] and Huete et al. [22] who conducted three-dimensional (3-D) LIA to study the interaction of a shock wave with an isotropic field of acoustic waves. Due to a lack of the precise nature of incident acoustic waves, previous studies of shock/acoustics interaction prescribed simplified forms of the energy spectrum for the incident acoustic field. Only second-moment statistics were examined using an isotropic energy spectrum while higher-order statistics that require information beyond the incoming energy spectrum were not studied. Quantitative comparisons of the 3D analysis with experiments or computations have not yet been conducted to validate the linear procedure due to a lack of datasets that are detailed enough to be suitable for comparison. The effects of the spectrum shape and the anisotropy of the inflow acoustic field have not been explored in existing LIA of shock/acoustics interaction.

Experiments have been carried out in wind tunnels and shock tubes with different means of generating incident turbulence or broadband disturbances [10, 23–27]. Existing techniques for generating incident turbulence include grids [24, 26], multi-tunnels [25], and laser photolysis [27]. As reviewed by Andreopoulos [28], it is very challenging to experimentally obtain a normal shock wave or a homogeneous turbulence field with the precise nature of inflow turbulence. Generating a homogeneous field of acoustic waves experimentally that is well characterized for studying shock/acoustics interaction is even more challenging, if possible. Experimental dataset of shock/acoustics interaction that are detailed enough to be suitable for theory validation or model development are still lacking.

DNS have been conducted extensively in the past two decades by multiple researchers for studying the interaction of a nominally normal shock wave with isotropic turbulence [4, 14, 29–37]. Previous studies were largely emphasized on the interaction between a spectrum of incident vorticity waves ("turbulence") with a plane shock wave. The additional effects of upstream thermodynamic fluctuations on shock/turbulence interaction (STI) were studied by either combining acoustic and/or entropy fluctuations into the upstream vortical field [14, 34] or considering compressible turbulence with a high turbulent Mach number [35, 37]. In nearly all previous DNS (except those by Ryu and Livescu [32]), the turbulent data at the upstream boundary of the computational domain were obtained from a pre-cursor DNS of time-decaying isotropic turbulence (IT), and the IT fields were advected through the inflow boundary of STI using Taylor's hypothesis. This hypothesis is questionable, however, for turbulence with significant acoustic mode contribution (i.e., dilatational turbulence) upstream of the shock [38]. To the knowledge of the authors, no existing DNS of STI have been conducted with the incident turbulence field dominated by acoustic waves or dilatational fluctuations. The lack of DNS studies is largely due to difficulties in generating a homogeneous field of acoustic waves with high degrees of physical realism for inflow conditions and the ambiguity with applying the Taylor's hypothesis for purely compressible motion such as dilatation [38]. As a results, the behaviors of shock/turbulence interaction in the pure dilatational limit is largely unknown.

The objective of this paper is to i) conduct DNS of shock/acoustics interaction to quantify significant flow characteristics and understand corresponding physical mechanisms associated with a homogeneous field of acoustic waves passing through a nominally normal shock wave; and ii) carry out comparative LIA to make distinctions between linear and nonlinear mechanisms. The DNS and LIA studies will help characterize the transfer function that converts post-shock flow disturbances to the pre-shock incident acoustic field, thereby providing insight into interpreting tunnel-noise data measured by an intrusive freestream probe.

The paper is structured as follows. The flow conditions and numerical methods are outlined in Section II. Results of DNS and LIA are presented in Section III. A summary of the planned work is given in Section IV.

II. Flow Conditions and DNS Methodology

The present work targets both DNS and LIA computations of a field of tunnel-like acoustic disturbances passing through a nominally normal shock wave. To emulate freestream acoustic disturbances in the test section of a two-dimensional supersonic wind tunnel, a precursor DNS of acoustic radiation from turbulent boundary layers developing spatially over interior walls of a supersonic Mach 2.5 channel was first conducted, and the flow conditions (including the unsteady acoustic disturbances) at the center of the channel were extracted and used for the primary simulation of shock-acoustics interaction. More details of the precursor DNS of the two-dimensional supersonic wind tunnel test section along with the methodology for extracting freestream acoustic disturbances will be introduced in Section II.A.3. Table 1 outlines the extracted preshock mean flow conditions used for the present work of of shock-acoustics interaction.

Table 1 Mean flow conditions upstream of the normal shock wave. Subscript "1" refers to quantities before the normal shock.

M_1	<i>U</i> ₁ (m/s)	$\rho_1 (\text{kg/m}^3)$	<i>T</i> ₁ (K)	$Re_u \times 10^6 (1/\text{m})$
2.5	823.2	0.1006	270.7	4.86

The pre-shock flow conditions match those in the free stream of an earlier two-dimensional tunnel DNS reported in [39, 40].

A. Direct Numerical Simulations

1. Governing Equations and Numerical Methods

The interaction between a homogeneous field of acoustic waves and a nominally normal shock wave is investigated through DNS. Here, DNS is referred to in the extended sense that all scales of turbulence and acoustic disturbances are resolved but the shock waves are captured numerically. Previous studies of canonical shock/turbulence interaction show that shock capturing schemes can accurately describe the shock-turbulence interaction process provided that the numerical shock thickness is much smaller than the smallest turbulence eddies or pressure structures (i.e., a separation of length scales exists between turbulence and shock wave) [30, 31, 33].

A high-order compressible-flow DNS solver, referred to as HyperWENO, is utilized for the current research. The compressible Navier-Stokes equations are solved with a hybrid scheme for the convective term. The 7th-order weighted essentially non-oscillatory (WENO) scheme [41] is used in the region around the shock invoked by a Ducros sensor [42] while a split central difference scheme [43] is used everywhere else in the domain. A 4th-order central difference scheme is used for the viscous flux terms, and a 3rd-order low storage Runge-Kutta scheme [44] is employed for time integration, which significantly relieves the memory requirement and is well suited for time-accurate simulations such as DNS.

The DNS code has been extensively tested and validated for computing both transitional and fully turbulent flows, including acoustic radiation of supersonic and hypersonic turbulent boundary layers [45, 46] and the interaction of freestream acoustic disturbances with a blunt cone [47]. A similar WENO method and WENO/central-difference hybrid method has been used in studying shock wave isotropic turbulence interactions [30, 31, 35].

2. Simulation Setup and Boundary Conditions

To numerically investigate the interaction of a tunnel-like acoustic disturbance field with a single plane shock wave, the DNS is set up with the inflow boundary of the computational domain lying upstream of the plane shock. "Tunnel-like" freestream acoustic disturbances are then introduced by prescribing flow variables at the inflow boundary based on the data saved from the precursor DNS of the disturbance environment inside a digital wind tunnel that pertains to an empty wind-tunnel configuration (i.e., without the test article). Fluctuation data within the freestream (i.e., supersonic core) region of the precursor DNS is extracted and, after necessary reconstruction, fed through the inlet boundary of the computational domain of the DNS involving the plane shock wave as schematically shown in Figure 2 (See Section II.A.3 for details of the tunnel-noise extraction process). Such an approach for prescribing inflow acoustic waves is free of numerical errors associated with the applications of the Taylor's hypothesis and/or the blending techniques commonly used for inflow turbulence generation in simulations of shock/vortical-turbulence interaction [38, 48, 49]. The incident acoustic field also has a high degree of physical realism as its genesis closely resembles that of the freestream acoustic disturbances in a conventional supersonic/hypersonic wind tunnel [5]. Periodic boundary conditions are imposed in transverse directions. At the outflow of the DNS, a sponge region similar to that of Larsson and Lele [30] is added to avoid acoustic reflections from the outflow boundary due to the subsonic flow behind the shock. The back-pressure at the outflow boundary is adjusted according to a linearized Rankine-Hugoniot relation for the pressure jump [30] until negligible shock drift is achieved and the normal shock remains essentially stationary.

The computational domain is selected to be large enough to contain most of the structures and also to allow post-shock flows to evolve into a equilibrium. The dimensions of the baseline DNS, referred to as M2p5DW, are listed in Table 2. Here, the domain sizes are measured in terms of the local tunnel-wall boundary-layer thickness $\delta = 7.4$ mm, which has been found to be the characteristic length scale of the large-scale acoustic structures radiated from the tunnel wall. Specifically, the thickness δ corresponds to $(k_{0,x}\delta, k_{0,y}\delta, k_{0,z}\delta) = (1.9\pi, 3.0\pi, 3.3\pi)$, where $(k_{0,x}, k_{0,y}, k_{0,z})$ are

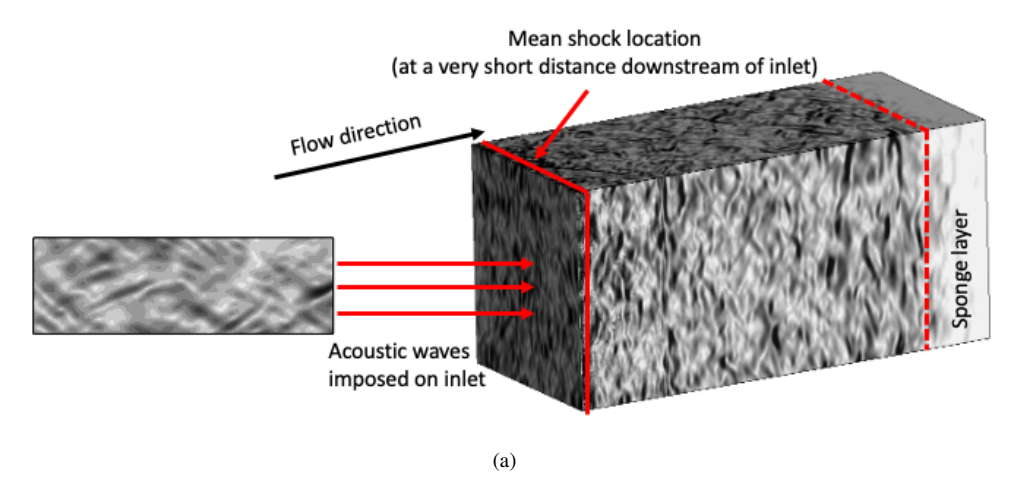


Fig. 2 Computational domain and simulation setup for DNS of shock/acoustics interaction.

Table 2 Domain sizes and grid resolutions of DNS of shock/acoustics interaction. The nominal location of the plane shock corresponds to $x \simeq 0$ m, and Δx_1 corresponds to the streamwise mesh resolution used in the precursor tunnel DNS. The reference length $\delta = 7.4$ mm is the local tunnel-wall boundary layer thickness at the location for extracting pre-shock acoustic disturbances, and the superscript "+" denotes normalization by the local viscous length $z_{\tau} = 15.22~\mu \text{m}$ of the local tunnel-wall boundary layer.

Case	$N_x \times N_y \times N_z$	x/δ	x_{sponge}/δ	$L_{ m y}/\delta$	L_z/δ	Δx_1^+	Δx_{shock}^+	Δx_2^+	Δy^+	Δz^+
M2p5DW	$2800 \times 276 \times 300$	-0.0026 - 3.9	3.9 - 5.9	2.9	2.6	8.55	0.00285	2.85	5.13	4.39
AI-2Dxz	$2800 \times 1 \times 300$	-0.0026 - 3.9	3.9 - 5.9	_	2.6	8.55	0.00285	2.85	-	4.39
AII-2Dxz	$4900 \times 1 \times 300$	-0.0026 - 5.6	5.6 - 7.6	_	2.6	8.55	0.00134	2.85	_	4.39
AIII-2Dxz	$2800 \times 1 \times 600$	-0.0026 - 3.9	3.9 - 5.9	_	2.6	8.55	0.00285	2.85	_	2.19
AIV-2Dxy	$2800 \times 276 \times 1$	-0.0026 - 3.9	3.9 - 5.9	2.9	-	8.55	0.00285	2.85	5.13	_
AV-2Dxy	$2800 \times 552 \times 1$	-0.0026 - 3.9	3.9 - 5.9	2.9	-	8.55	0.00285	2.85	2.57	_

the peak streamwise and transverse wavenumbers of the pre-multiplied pressure spectra upstream of the shock. Similar to the previous work of shock/vortical-turbulence interaction by Larsson and Lele [30], the mesh for the current work is distributed uniformly in the two transverse directions and is stretched in the longitudinal direction to provide better streamwise resolution at the shock. Considering that the previous work found that shock/vortical-turbulence interaction can lead to a reduction in post-shock spatial scales [30], a systematical grid convergence study has been conducted for the present work to find a reasonable resolution that balances accuracy and computational cost. Specifically, the dependence of numerical results on grid resolution is investigated by a series of auxiliary DNS listed in Table 2, where Case M2p5DW is the baseline simulation, and the other five cases are auxiliary DNS with refined grids that simulate shock/acoustics interaction in a two-dimensional slice of the baseline domain, which are oriented in the x-y and x-z plane, respectively. All cases are identical in terms of numerical method, computational setup, and flow conditions excepted for the parameters listed in Table 2. Figure 3 compares some of the transfer functions for DNS solutions corresponding to each of the three cases. All curves collapse to within 0.8%, indicating good grid convergence for the quantities of interest.

As additional risk-reduction effort, Figure 4 compares the transfer functions of DNS (with baseline resolution) and LIA for the interaction of a normal shock wave with a single plane slow acoustic wave at different wave angles (Figure 4). Very good agreement is achieved between DNS and LIA, which further confirms the validity of the current numerical setup and grid resolution.

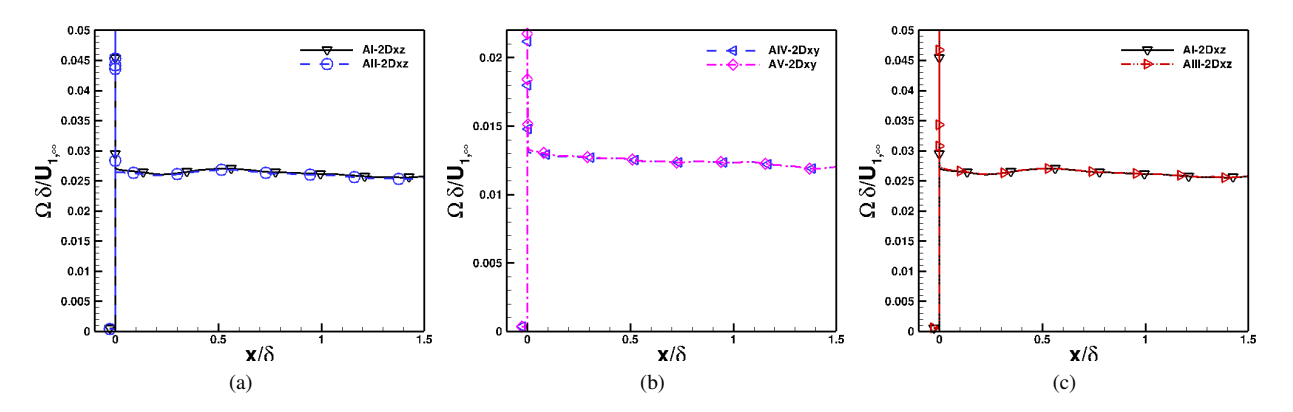


Fig. 3 Grid convergence of the mean vorticity magnitude Ω conducted in two-dimensional domains of different grid resolutions.

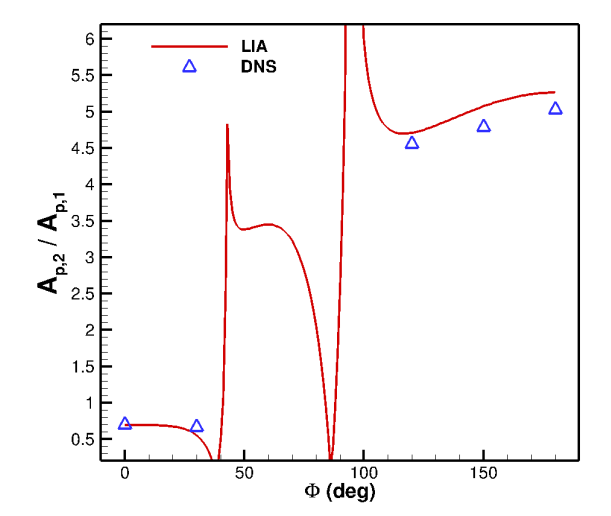


Fig. 4 Amplification of pressure fluctuation magnitude $A_{p,2}/A_{p,1}$ predicted by DNS (with baseline resolution) and LIA for the interaction of a normal shock wave with a single plane slow acoustic wave at different wave angles at Mach 2.5.

3. "Tunnel-like" Acoustic Disturbance Generation and Extraction

To generate a field of "tunnel-like" acoustic disturbances that interacts with a normal shock, a precursor DNS of a spatially evolving channel flow at Mach 2.5 was conducted to simulate the acoustic radiation from the tunnel-wall turbulent boundary layers within a rectangular test section of a supersonic wind tunnel. The emphasis is on extracting the radiated pressure fluctuations in the core region of the test section. Figure 5a shows the computational setup of the precursor simulation of the channel-shaped test section at Mach 2.5. The test section has a slightly increasing height with an expansion angle of 0.3 deg to account for a growing boundary layer downstream, and a comparison in turbulence statistics of the channel-wall turbulent boundary layers against those of a single-wall flat plate has confirmed that the resulting Clauser pressure-gradient parameter is negligibly small over the downstream portion of the channel where statistics of acoustic fields are evaluated, and a near-equilibrium state have been reached in the channel-wall turbulent boundary layers. By choosing such a channel geometry, the effects of surface curvature and pressure gradient in the streamwise direction can be neglected to the leading order, thus avoiding extraneous complexity in the simulation. To generate the inflow boundary conditions for the channel case, two independent, spatially developing single-wall boundary layers are first simulated, and the time series profiles extracted from each single-wall simulation are imposed

as the inflow boundary conditions for the turbulent boundary layer developing over either the top or bottom wall of the channel. Additional details of the channel DNS can be found in Prasad et al. [39] and Goparaju et al. [40]. Figure 5b shows an instantaneous visualization of the density gradient associated with the radiated acoustic field in the Mach 2.5 wind tunnel predicted by the precursor DNS. Near the walls, coherent turbulent fluctuations arise and radiate pressure waves into the center of the test section. Within the supersonic core of the test section, the prominent structures associated with acoustic fluctuations are shown to consist of both upward and downward propagating acoustic waves, indicating contributions to the local acoustic radiation from the boundary layers along the bottom and top walls, respectively. The inclination angle of the downward inclined pressure structures radiating from the bottom wall boundary layer is approximately 40°, which is nearly the same as that of a single-wall case reported by Duan et al. [45]. The spatiotemporal structures of these freestream acoustic fields are extracted next and used as the inflow boundary condition for the DNS of shock-acoustics interaction.

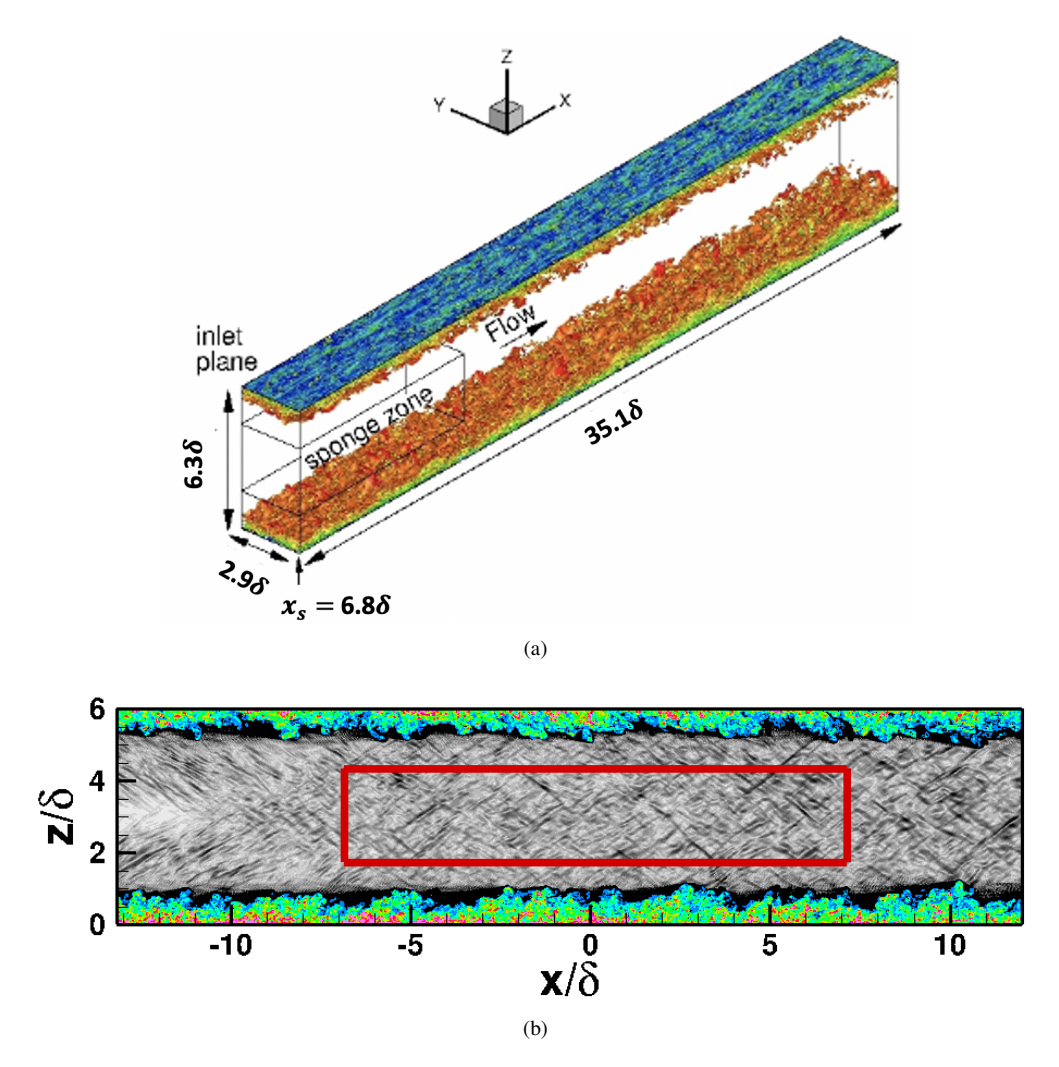


Fig. 5 (a) Computational domain set up for the precursor DNS of two-dimensional channel test section at Mach 2.5 [39]; (b) Numerical schlieren images (i.e., density gradient contours) of radiated acoustic waves within the supersonic core of the test section. The reference length of $\delta = 7.4$ mm is local boundary layer thickness of tunnel-wall boundary layers.

For extracting the freestream acoustic field from the precursor DNS of a two-dimensional supersonic test section, we represent the acoustic perturbations outside of the tunnel-wall turbulent boundary layers as the superposition of a large number of plane wave components:

$$\begin{bmatrix} p'_{1} \\ \rho'_{1} \\ u'_{1} \\ v'_{1} \\ w'_{1} \\ T'_{1} \end{bmatrix} = \sum_{j=1}^{N} \begin{bmatrix} \frac{1}{\frac{1}{\bar{c}_{1}^{2}}} \\ \frac{1}{\bar{\rho}_{1}\bar{c}_{1}} \left(\frac{k_{x,j}}{\|\mathbf{k}_{j}\|} \right) \\ \frac{1}{\bar{\rho}_{1}\bar{c}_{1}} \left(\frac{k_{y,j}}{\|\mathbf{k}_{j}\|} \right) \\ \frac{1}{\bar{\rho}_{1}\bar{c}_{1}} \left(\frac{k_{z,j}}{\|\mathbf{k}_{j}\|} \right) \\ \frac{1}{\bar{\rho}_{1}\bar{c}_{1}} \left(\frac{k_{z,j}}{\|\mathbf{k}_{j}\|} \right) \\ \frac{(\gamma-1)\overline{T}_{1}}{\gamma\overline{\rho}_{1}} \end{bmatrix}$$

$$(1)$$

Here, $\mathbf{x}=(x,y,z)$ denotes the vector of Cartesian spatial coordinates, $(\cdot)_1'$ denotes the perturbations with respect to the mean freestream quantities, and "c.c." stands for complex conjugate. The quantities $\mathbf{k}_j=(k_{x,j},k_{y,j},k_{z,j}), \omega_j, \hat{p}_j,$ and ϕ_j represent the wavenumber vector, angular frequency, complex amplitude, and phase, respectively, of the plane acoustic wave with index j. The norm of the wavenumber vector is defined as $\|\mathbf{k}_j\| \equiv \sqrt{k_{x,j}^2 + k_{y,j}^2 + k_{z,j}^2}$. The angular frequency ω_j of the jth wave is related to its wavenumber \mathbf{k}_j via the dispersion relation for acoustic waves [50]:

$$\omega_j(\mathbf{k}_j) = \overline{\mathbf{u}}_1 \cdot \mathbf{k}_j \pm \overline{c}_1 \|\mathbf{k}_j\|, \tag{2}$$

The corresponding group velocity $\overline{\mathbf{v}}_i$ of the acoustic waves can be written as:

$$\overline{\mathbf{v}}_{\pm,j} \equiv \frac{\partial \omega_j}{\partial \mathbf{k}_j} = \overline{\mathbf{u}}_1 \pm \overline{c}_1 \left(\frac{\mathbf{k}_j}{\|\mathbf{k}_j\|} \right). \tag{3}$$

The plus-minus sign (\pm) in Eq. (3) indicates that the group velocity of the acoustic waves can be faster or slower than the mean flow velocity $\overline{\mathbf{u}}_1$, with the relative magnitude (with respect to the mean flow) equal to the speed of sound \overline{c}_1 along the wave front orientation $\mathbf{k}_j/\|\mathbf{k}_j\|$. Here, we follow the definition of McKenzie and Westphal [50] by referring to acoustic waves with $\overline{\mathbf{v}}_{+,j} = \overline{\mathbf{u}}_1 + \overline{c}_1\left(\frac{\mathbf{k}_j}{\|\mathbf{k}_j\|}\right)$ as the "fast" acoustic waves and those with a group speed of $\overline{\mathbf{v}}_{-,j} = \overline{\mathbf{u}}_1 - \overline{c}_1\left(\frac{\mathbf{k}_j}{\|\mathbf{k}_j\|}\right)$ as "slow" acoustic waves.

Given a tunnel operating condition with known time-averaged freestream quantities, the information required to complete the specification of the acoustic field according to the plane-wave model in Eq. (1) corresponds to the parameters \mathbf{k}_i , \hat{p}_i , ϕ_i and making a choice between fast and slow waves or a mixture thereof.

To determine the unknown parameters in Eq. 1 that are required to synthesize the broadband field of three-dimensional acoustic disturbances in the free stream region from the tunnel DNS as visualized in Figure 5b, we first extract the instantaneous pressure field within a rectangular domain from the freestream region of the precursor DNS. The size of the rectangular domain relative to the tunnel boundary layer thickness is approximately $(L_x/\delta, L_y/\delta, L_z/\delta) = (14.1, 2.9, 2.6)$ and includes a total of (800, 276, 150) points in the streamwise and the two transverse directions, respectively, from the precursor DNS (Figure 6). Here, $\delta = 7.4$ mm represents the tunnel-wall boundary layer thickness at x = 0 (i.e., around the location of the plane shock wave in shock/acoustics interaction). The selected domain for acoustic wave extraction is large enough to accommodate the largest freestream acoustic structures. After a detrending process to compute the acoustic pressure fluctuations p'_1 by subtracting the mean pressure \overline{p}_1 , spatial fast Fourier transforms (FFT) are performed along each spatial direction of the rectangular domain. This provides the specification of the modal content of the acoustic fluctuations, including the wavenumber vector $\mathbf{k}_j = (k_{x,j}, k_{y,j}, k_{z,j})$, complex amplitude \hat{p}_j , and the phase angle ϕ_j for each individual mode j. Given the wavenumber vector \mathbf{k}_j of each mode j, its frequency can be computed by Eq. 2 with the assumption of a slow acoustic wave. The dominance of slow acoustic waves (with a propagation speed slower than the sound speed) in the free stream of conventional supersonic and hypersonic tunnels has been suggested in multiple previous studies [12, 40, 45, 46], and will be further confirmed next for the current two-dimensional tunnel test section. To guarantee that only statistically relevant modes are kept in the synthesized acoustic field, the three-dimensional spatial fast Fourier transform (FFT) is repeated within the same rectangular domain for a total of $N_f = 60$ snapshots of the instantaneous freestream acoustic fields, and the modal amplitudes \hat{p}_i in the acoustic model from Eq. 1 are computed by using an average of the power spectral densities across the snapshots. However, to preserve the stochasticity of the reconstructed field, the phase angles (ϕ_i) in the acoustic model are derived from a single instantaneous snapshot of the extracted three-dimensional acoustic field. Additionally, because the split central difference scheme used for the tunnel DNS requires approximately 8 points per wavelength to accurately

propagate a linear wave over multiple wavelengths, a low-pass wavenumber filter with spectral cut-off is applied to remove the small-wavelength waves that cannot be accurately resolved by the precursor DNS. To be conservative, we have also excluded any acoustic wave components that have frequencies higher than 1 MHz, which cannot be resolved with the given mesh resolution of the precursor DNS. The total number of plane waves included in the acoustic-wave ansats is $N \approx 65000$.

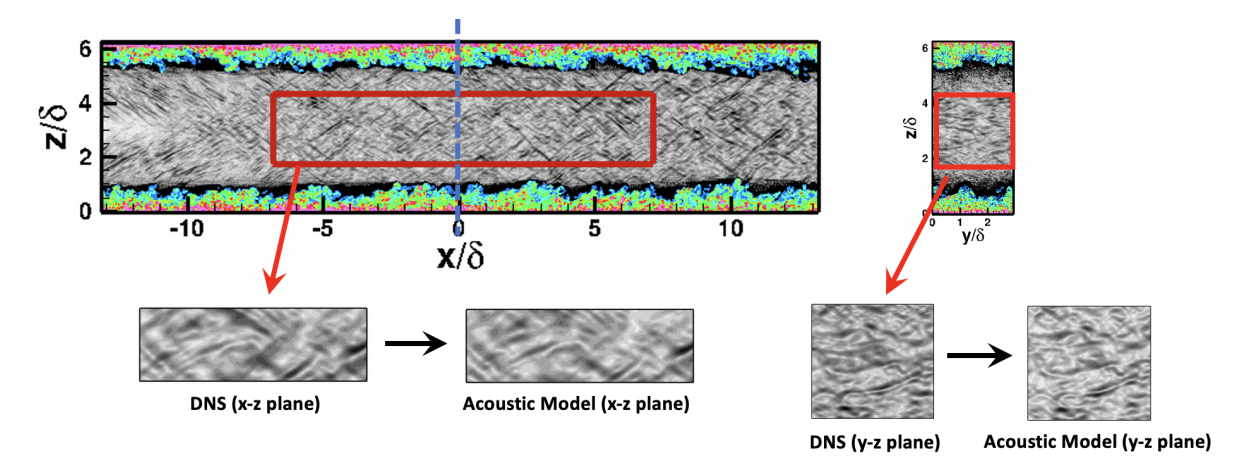


Fig. 6 Schematic of the rectangular domain for extracting freestream acoustic disturbances from the precursor DNS of empty wind tunnel. The vertical dashed line indicates the streamwise location of the selected cross-plane visualized on the top right.

To assess the effectiveness of the acoustic disturbance model, Figure 7 plots the power spectral density (PSD) of freestream acoustic disturbances computed based on the calibrated acoustic model of Eq. 1 with fast (+) or slow (-) acoustic wave assumptions in comparison with that of the precursor tunnel DNS. Very good agreement is achieved between the acoustic model with the slow-acoustic-wave assumption and the DNS data, reconfirming the dominance of slow acoustic waves in the radiated noise from the tunnel-wall turbulent boundary layer.

Figure 8 compares the wavenumber and frequency spectra of freestream acoustic disturbances computed based on the calibrated acoustic model of Eq. 1 with different spatial domains for acoustic extraction against those of the precursor tunnel DNS. Here, the rectangular domain sizes are measured in terms of the local tunnel boundary-layer thickness δ_{tunnel} and the wavenumber and frequency spectra of both pressure and streamwise velocity fluctuations are included to show the sensitivity of different acoustic quantities to the model parameters. With the selected domain size of $(L_x/\delta, L_y/\delta, L_z/\delta) = (14.1, 2.9, 2.6)$ for extracting the freestream acoustic waves, excellent comparisons between the model and the DNS are achieved in spectra of both pressure and velocity fluctuations. A further comparison among model predictions with different domain sizes suggests that the model-predicted frequency spectrum is insensitive to the longitudinal and transverse extents of the domain, while a large enough domain size in the transverse directions is indeed required for the model-predicted wavenumber spectra to match with the tunnel DNS.

Figure 9 visualizes the temporal evolution of freestream acoustic disturbances in a flow-parallel-plane (x-z plane) generated by the calibrated acoustic model of Eq. 1 in comparison with those from the precursor tunnel DNS. Here, the freestream acoustic disturbances are visualized by the numerical schlieren (i.e., density gradient contours). The visualization at t = 0 corresponds to the snapshot from which the modal phase ϕ_j of all the plane waves in the ansats are derived, and the time delay is measured in terms of the integral time scale Λ of the freestream pressure disturbances. The apparent similarity in the instantaneous acoustic structures between the model and DNS confirms that the freestream acoustic disturbances generated from the acoustic model closely mimic those of the DNS over at least multiple integral time scales Λ , and the stochasticity of the freestream acoustic field is also very well preserved by the model.

The tunnel-noise generation technique in the Cartesian domain has been extended to the cylindrical domain and is shown to be effective for studying boundary layer transition over a circular cone model in a hypersonic wind tunnel with an axisymmetric nozzle [47].

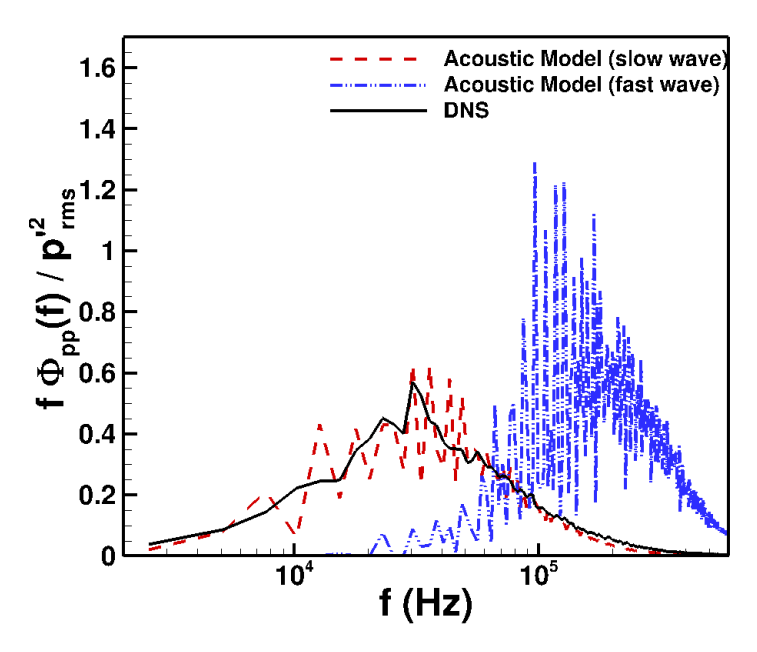


Fig. 7 PSD of freestream acoustic disturbances computed based on the calibrated acoustic model of Eq. 1 with fast (+) or slow (-) acoustic wave assumptions in comparison with that of the precursor tunnel DNS.

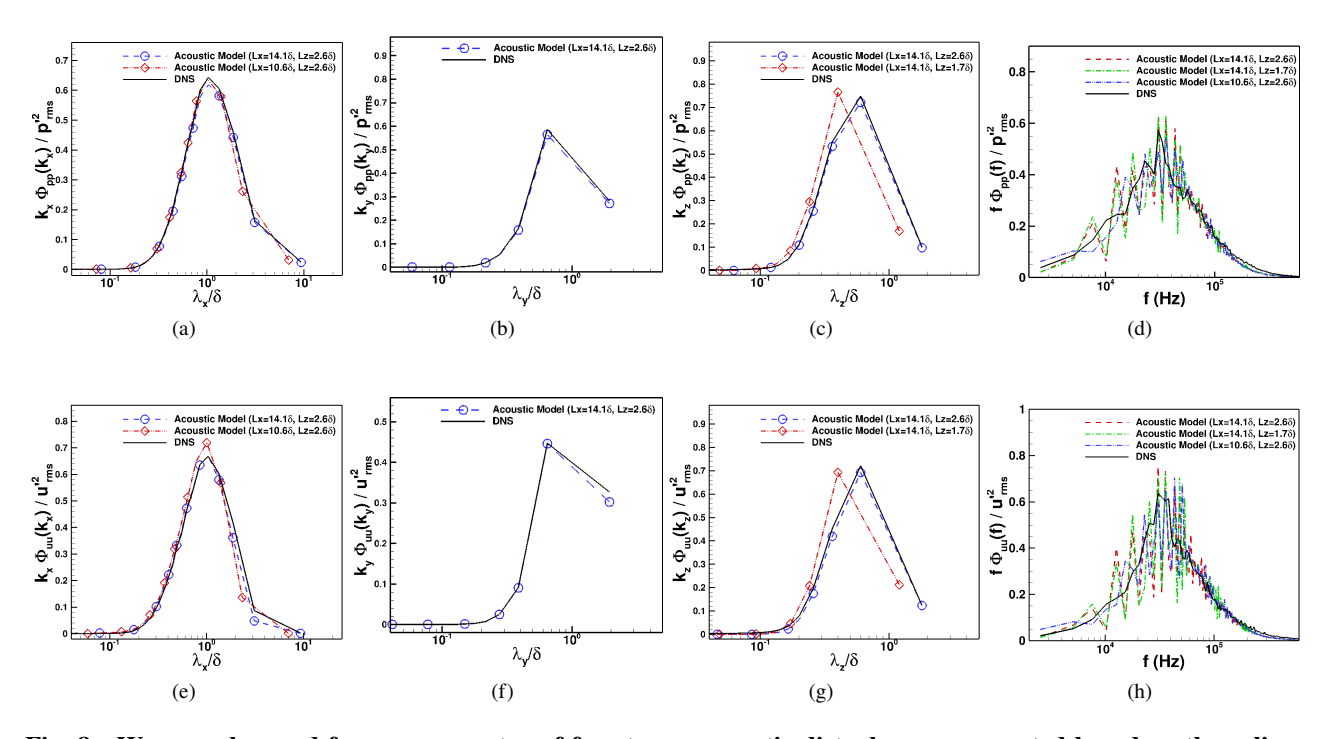


Fig. 8 Wavenumber and frequency spectra of freestream acoustic disturbances computed based on the calibrated acoustic model of Eq. 1 with different spatial domain sizes in comparison with those of the precursor tunnel DNS. (a-d) pressure and (e-h) streamwise velocity. The domain size for extracting freestream acoustic is normalized by local tunnel boundary-layer thickness of $\delta = 7.4$ mm).

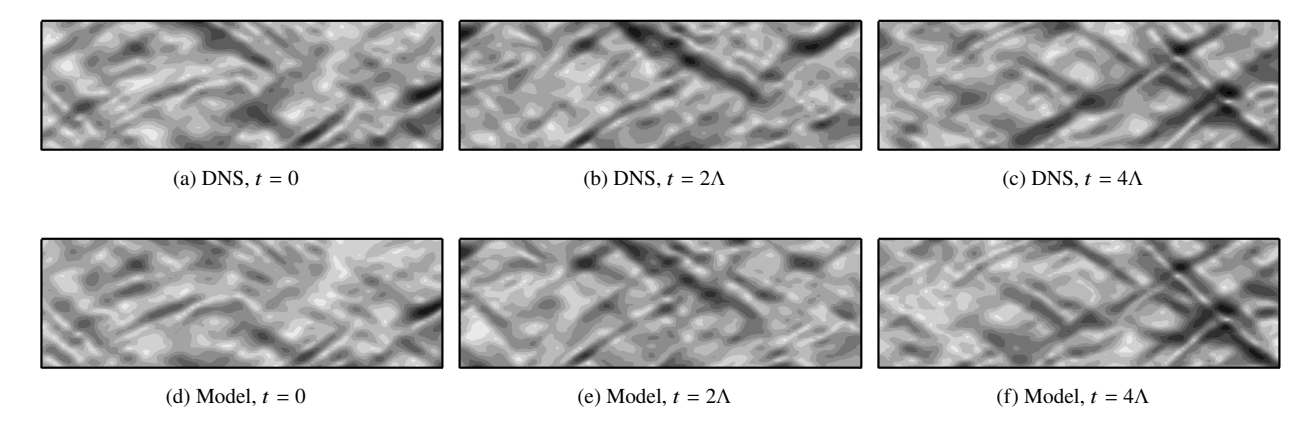


Fig. 9 Temporal evolution of freestream acoustic disturbances in a flow-parallel-plane (x-z plane) generated by the calibrated acoustic model of Eq. 1 in comparison with those from the precursor tunnel DNS. Here, the freestream acoustic disturbances is visualized by the numerical schlieren (i.e., density gradient contours) and the time delay is measured in terms of the integral time scale $\Lambda = 4.8 \ \mu s$ of the freestream acoustic disturbances.

B. Linear Interaction Analysis

In the present work, LIA is performed use the same incident acoustic fields as the DNS, and comparisons are made between LIA and DNS to understand the validity of LIA for predicting the transfer function for propagating tunnel-like acoustic disturbance field across a plane shock wave as well as to distinguish between linear and nonlinear interaction mechanisms. Specifically, the tunnel-like acoustic field in front of the shock wave are specified according to an ansatz of slow plane acoustic waves of Eq. 1. Each plane acoustic mode is assumed to interact independently with the shock wave and generate downstream disturbances according to the solutions of Moore [3] and Mahesh et al. [15]. A superposition of the downstream waves induced by each incident acoustic wave gives statistics of the disturbances behind the shock wave. A similar procedure was initially proposed by Mahesh et al. [15] for an isotropic field of acoustic waves.

III. Results

In this section, results of DNS and LIA for shock/acoustics interaction with tunnel-like incident acoustic disturbances at $M_1 = 2.5$ are presented.

Figure 10 shows the streamwise variation of turbulence kinetic energy (TKE) $q = \overline{u_k' u_k'}/2$ as predicted by DNS and LIA. The shock is located at x = 0, and the TKE is normalized by its upstream value to highlight the amplification of disturbance levels due to shock/acoustics interaction. The streamwise distance is normalized by the local tunnel-wall boundary layer thickness δ , which is the similar to the peak streamwise wavelength $\lambda_{x,pk} = 2\pi/k_{0,x}$ of the upstream acoustic disturbances (Figure 8a). Behind the shock, there is an adjustment region of length $L_a \approx 0.5\delta$ wherein the TKE shows a rapid non-monotonic near-field variation, followed by the far-field in which both the DNS and LIA predictions are constant. Although the LIA slightly underpredicts the exponential decay immediately behind the shock, it is in good agreement with the DNS in the far-field.

Figure 11 further shows the evolution of the Reynolds normal stresses $(\overline{u'u'}, \overline{v'v'}, \overline{w'w'})$ behind the shock. The LIA predicts the non-monotonic variation of the Reynolds stresses in the near-field and the DNS results are in good agreement with this. In the far-field, however, the LIA predicts lower intensity of the streamwise component $\overline{u'u'}$ but increased magnitudes of the transverse components $(\overline{v'v'}, \overline{w'w'})$ than the DNS. A similar over-prediction of the transverse components of the Reynolds stresses by LIA has been reported by Larsson et al. [31] in their study of canonical shock/vortical-turbulence interaction.

Figure 12 shows the evolution of the static pressure variance $\overline{p'^2}$ behind the shock wave as predicted by DNS and LIA. There is an exponential decay in $\overline{p'^2}$ immediately behind the shock that is well predicted by LIA. In the far-field, the DNS gives a constant level associated with the propagating acoustic waves and the LIA results are in very good agreement with the DNS. A similar exponential decay of $\overline{p'^2}$ in the near-field and a similarly good comparison between DNS and LIA have been reported by Quadros et al. [18] for canonical shock/vortical-turbulence interaction.

Figure 13 shows the DNS-predicted power spectral density (PSD) for static pressure (p'_2) and total pressure $p'_{t,2}$ at

multiple post-shock locations. For reference, the PSD for the pre-shock static pressure (p_1') is added to highlight any deviation from the upstream reference value. Additionally, to highlight the distribution of disturbance energy among different frequencies, each of the spectrum curves is normalized by the corresponding power values $(p_{rms}'^2)$ or $p_{t,rms}'^2$ so that the area underneath the spectrum curve is unity. The PSD of post-shock static pressure p_2' shows significant deviation from the pre-shock value at high frequencies in the near-field but it recovers to the pre-shock value in the far-field $(x/\delta \gtrsim 0.5)$. For post-shock total pressure $p_{t,2}'$, however, the PSD seems to be similar to that of the pre-shock static pressure p_1' at all locations. Further study with a longer signal length and better statistical convergence will be performed to confirm the trend.

Finally, Figure 14 shows the DNS-predicted spatial correlation coefficient of the static pressure p'_2 in multiple cross-planes behind the shock. While the post-shock pressure structures are significantly skewed in the near-field, these structures become more isotropic over the cross-plane in the far-field. Shock/acoustics interaction leads to a significant increase in the structure sizes along the two transverse directions.

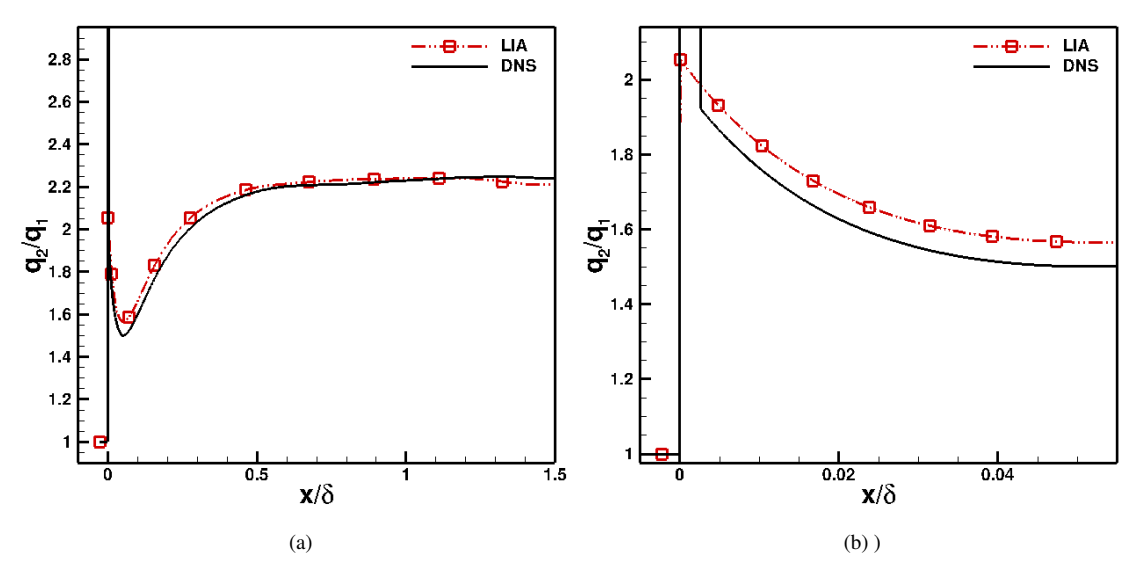


Fig. 10 Evolution of the turbulent kinetic energy $q = \overline{u_k' u_k'}/2$ behind the shock wave as predicted by DNS and LIA.

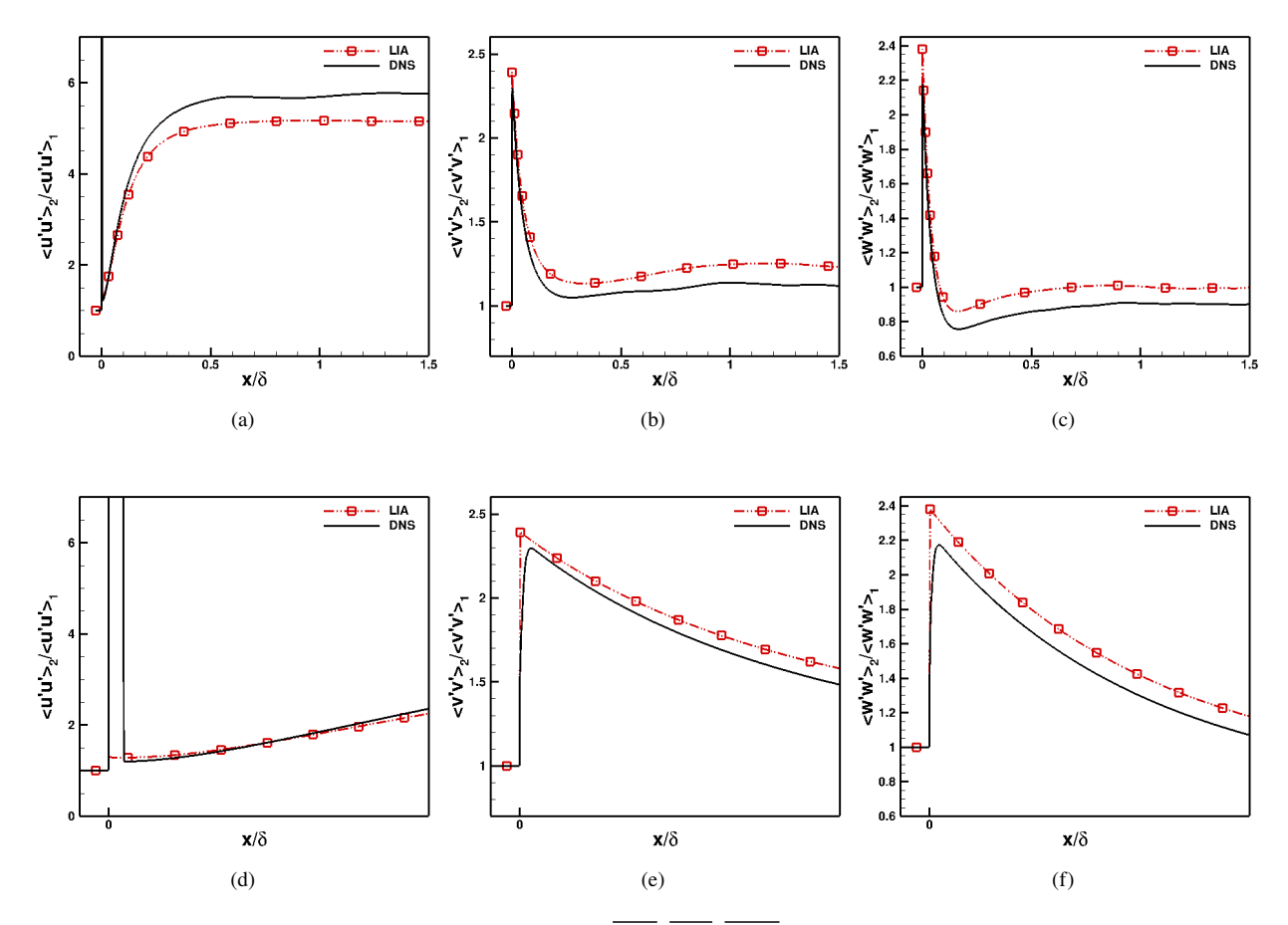


Fig. 11 Evolution of the Reynolds normal stresses $(\overline{u'u'}, \overline{v'v'}, \overline{w'w'})$ behind the shock wave as predicted by DNS and LIA.

IV. Summary

In this paper, direct numerical simulation (DNS) and linear interaction analysis (LIA) were performed to study shock/acoustics interaction with tunnel-like incident acoustic disturbances. The acoustic field was extracted from a pre-cursor DNS that simulates the test section of a Mach 2.5 digital wind tunnel. he paper first presented a systematic methodology for extracting and reconstructing broadband acoustic disturbances radiated from the tunnel-wall turbulent boundary layer. The study found that the broadband tunnel noise in the free stream (i.e., outside of the tunnel-wall turbulent boundary layer) can be well represented by an acoustic model based on a plane wave decomposition comprised of a large number of planar, slow acoustic waves. With successful calibration of the model parameters against the precursor tunnel DNS, the acoustic model can successfully reproduce the frequency and wavenumber spectra of the broadband tunnel noise. Additionally, the temporal evolution of the stochastic acoustic structures is well captured by the calibrated model. Given the analytical nature of the derived acoustic model, the time-series data generated according to such a model can be readily imposed as the inflow boundary of the DNS or as the input of LIA for studying shock/acoustics interaction.

Next, the paper presented DNS and LIA results of shock/acoustics interaction. The study found that a good comparison in the TKE and pressure fluctuation variance $\overline{p'^2}$ behind the shock was achieved between DNS and LIA. These quantities undergo rapid non-monotonic variation just behind the shock over an adjustment region of length $L_a \approx 0.5\delta$, followed by the far-field in which both the DNS and LIA predictions are constant. An over-prediction of the transverse components of the Reynolds stresses by LIA was found in the post-shock region, which is similar to that reported by Larsson et al. [31] in their study of canonical shock/vortical-turbulence interaction. The PSD of post-shock static pressure p'_2 predicted by DNS shows significant deviation from the pre-shock value at high frequencies

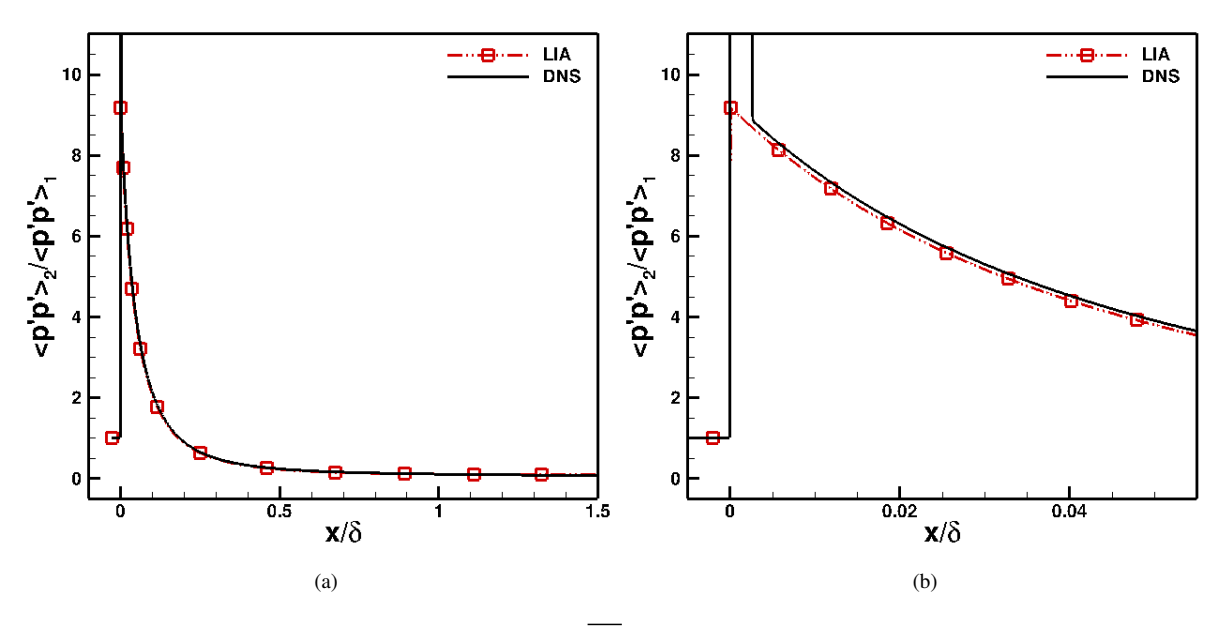


Fig. 12 Evolution of the static pressure variance $\overline{p'^2}$ behind the shock wave as predicted by DNS and LIA.

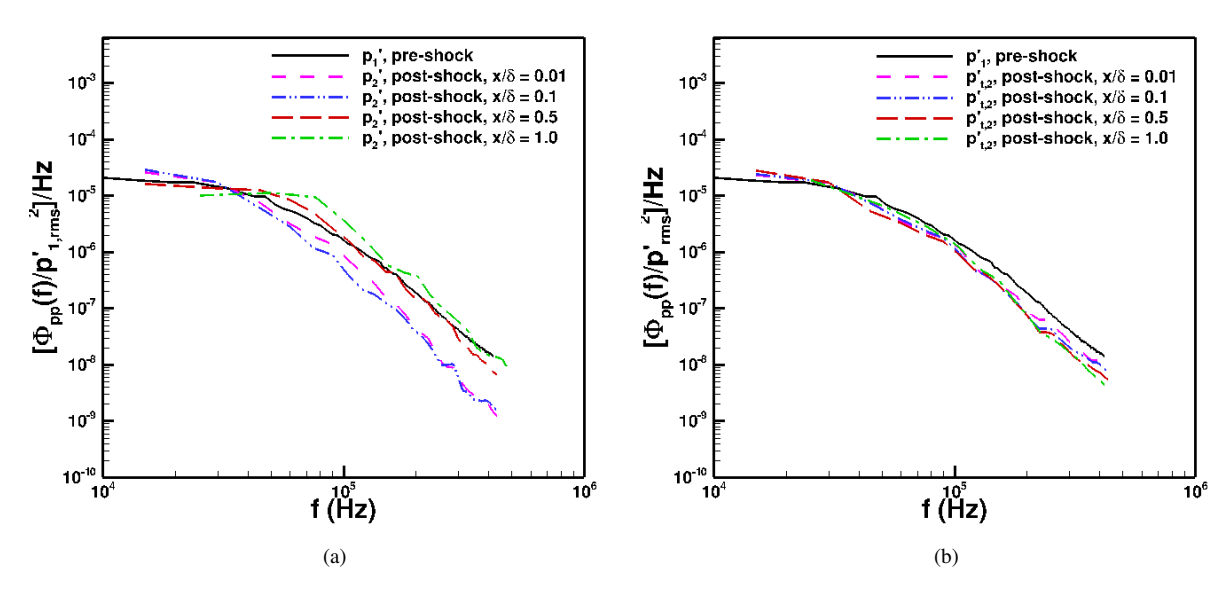


Fig. 13 Power spectral density predicted by DNS at multiple post-shock locations. (a) post-shock static pressure p'_2 ; (b) post-shock total pressure $p'_{t/2}$.

in the near-field but it recovers to the pre-shock value in the far-field $(x/\delta \gtrsim 0.5)$, while the PSD of the post-shock total pressure $p'_{t,2}$ is found to be similar to that of the pre-shock static pressure p'_1 in both near-field and far-field. The DNS-predicted spatial correlation coefficient shows that shock/acoustics interaction leads to a significant increase in the structure sizes along the two transverse directions.

Ongoing and future work includes additional data analysis and more detailed comparisons between DNS and LIA for predicting the transfer function of shock/acoustics interaction, with an emphasis on assessing theoretical tools such as LIA to provide reasonable approximations. The study will also be extended to include comparisons in transfer functions

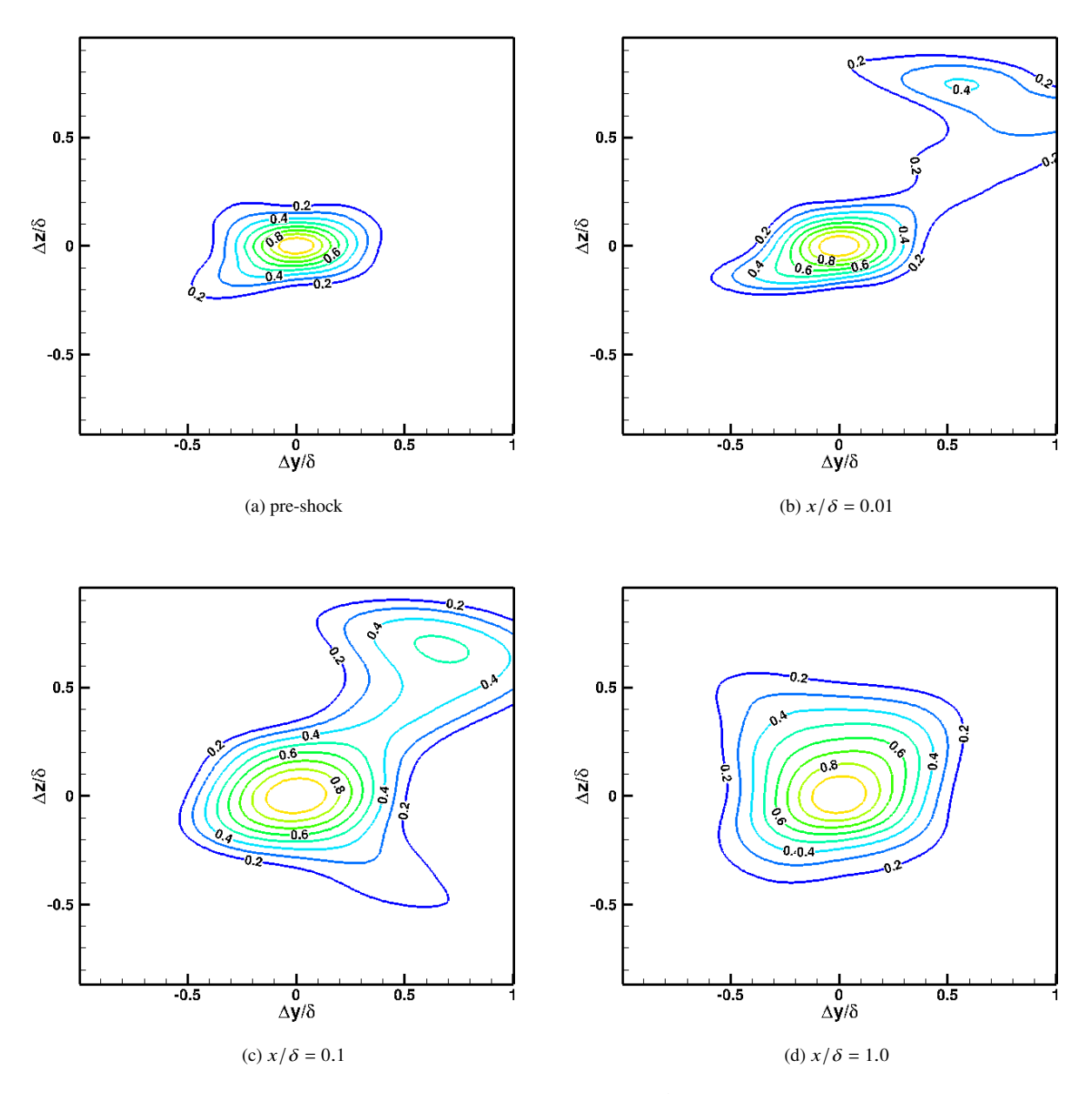


Fig. 14 Spatial correlation coefficient of the static pressure p'_2 in multiple cross-planes behind the shock predicted by the DNS.

among incident acoustic fields of different spectra.

Acknowledgments

This material is based upon work supported by the National Science Foundation under Grant No. CBET 2001125, managed by Dr. Ron Joslin. Computational resources were provided by the Ohio Supercomputer Center. Any opinions, findings, and conclusions or recommendations expressed in this material are those of the author(s) and do not necessarily reflect the views of the National Science Foundation.

References

- [1] Kovasznay, L. S. G., "Turbulence in Supersonic Flow," *Journal of Aeronautical Sciences*, Vol. 20, 1953, pp. 657-674. https://doi.org/10.2514/8.2793.
- [2] Ribner, H. S., "Convection of a Pattern of Vorticity through a Shock Wave," Tech. Rep. 2864, NACA TN, 1953.
- [3] Moore, F. K., "Unsteady Oblique Interaction of a Shock Wave with a Plane Disturbance," Tech. Rep. 1165, National Advisory Committee for Aeronautics (NACA), 1954.
- [4] Lee, S., Lele, S. K., and Moin, P., "The Interaction of a Shock Wave with a Turbulent Shear Flow," Tech. Rep. 69, Thermosciences Division, Department of Mechanical Engineering, Stanford University, 1996.
- [5] Laufer, J., "Some Statistical Properties of the Pressure Field Radiated by a Turbulent Boundary Layer," *Physics of Fluids*, Vol. 7, No. 8, 1964, pp. 1191–1197. https://doi.org/10.1063/1.1711360.
- [6] Stetson, K. F., "Nosetip Bluntness Effects on Cone Frustrum Boundary-Layer Transition in Hypersonic Flow," *AIAA Paper 83-1763*, 1983. https://doi.org/10.2514/6.1983-1763.
- [7] Bushnell, D. M., "Notes on Initial Disturbance Fields for the Transition Problem," *Instability and Transition, edited by M. Y. Hussaini and R. G. Voigt, Springer-Verlag, Berlin*, Vol. 1, 1990, pp. 217–232.
- [8] Bounitch, A., Lewis, D. R., and Lafferty, J. F., "Improved Measurements of "Tunnel Noise" Pressure Flucutations in the AEDC Hypervelocity Wind Tunnel No. 9," *AIAA Paper 2011-1200*, 2011. https://doi.org/10.2514/6.2011-1200.
- [9] Masutti, M., Chazot, E., and Carbo, M., "Disturbance Level Characterization of a Hypersonic Blow-Down Facility," *AIAA Journal*, Vol. 50, No. 12, 2012, pp. 2720–2730. https://doi.org/10.2514/1.J051502.
- [10] Mai, C. L. N., and Bowersox, R. D., "Effect of a Normal Shock Wave on Freestream Total Pressure Fluctuations in a Low-Density Mach 6 Flow," AIAA Paper 2014-2641, 2014. https://doi.org/10.2514/6.2014-2641.
- [11] Schilden, T., Schröder, W., Ali, S. R. C., Schreyer, A. M., Wu, J., and Radespiel, R., "Analysis of Acoustic and Entropy Disturbances in a Hypersonic Wind Tunnel," *Physics of Fluids*, Vol. 28, 2016, p. 056104. https://doi.org/10.1063/1.4948435.
- [12] Duan, L., Choudhari, M. M., Chou, A., Munoz, F., Ali, S. R. C., Radespiel, R., Schilden, T., Schröder, W., Marineau, E. C., Casper, K. M., Chaudhry, R. S., Candler, G. V., Gray, K. A., and Schneider, S. P., "Characterization of Freestream Disturbances in Conventional Hypersonic Wind Tunnels," *Journal of Spacecraft and Rockets*, Vol. 56, No. 2, 2019, pp. 357–368. https://doi.org/10.2514/1.A34290.
- [13] Beckwith, I. E., and Miller, C. G., "Aerothermodynamics and Transition in High-Speed Wind Tunnels at Nasa Langley," *Annual Review of Fluid Mechanics*, Vol. 22, 1990, pp. 419–439. https://doi.org/10.1146/annurev.fl.22.010190.002223.
- [14] Mahesh, K., Lee, S., Lele, S. K., and Moin, P., "The Influence of Entropy Fluctuations on the Interaction of Turbulence with a Shock Wave," *Journal of Fluid Mechanics*, Vol. 340, 1997, pp. 225–247. https://doi.org/10.1017/S0022112097004576.
- [15] Mahesh, K., Lee, S., Lele, S. K., and Moin, P., "The Interaction of an Isotropic Field of Acoustic Waves with a Shock Wave," *Journal of Fluid Mechanics*, Vol. 300, 1995, pp. 383–407. https://doi.org/10.1017/S0022112095003739.
- [16] Fabre, D., Jacquin, L., and Sesterhenn, J., "Linear Interaction of a Cylindrical Entropy Spot with a Shock," *Physics of Fluids*, Vol. 13, No. 8, 2001, pp. 2403–2422. https://doi.org/10.1063/1.1383592.
- [17] Wouchuk, J. G., Lira, D., Huete, C., and Velikovich, A. L., "Analytical Linear Theory for the Interaction of a Planar Shock Wave with an Isotropic Turbulent Vorticity Field," *Physical Review E*, Vol. 79, 2009, p. 066315. https://doi.org/10.1103/PhysRevE.79.066315.
- [18] Quadros, R., Sinha, K., and Larsson, J., "Turbulent Energy Flux Generated by Shock/Homogeneous-Turbulence Interaction," *Journal of Fluid Mechanics*, Vol. 796, 2016, pp. 113–157. https://doi.org/10.1017/jfm.2016.236.
- [19] Durbin, P. A., and Zeman, O., "Rapid Distortion Theory for Homogeneous Compressed Turbulence with Application to Modeling," *Journal of Fluid Mechanics*, Vol. 242, 1992, pp. 349–370. https://doi.org/10.1017/S0022112092002404.
- [20] Jacquin, L., Cambon, C., and Blin, E., "Turbulence Amplification by a Shock Wave and Rapid Distortion Theory," *Physics of Fluids*, Vol. 5, No. 10, 1993, pp. 2539–2550. https://doi.org/10.1063/1.858767.

- [21] Cambon, C., Coleman, G. N., and Mansour, N. N., "Rapid Distortion Analysis and Direct Simulation of Compressible Homogeneous Turbulence at Finite Mach Number," *Journal of Fluid Mechanics*, Vol. 257, 1993, pp. 641–665. https://doi.org/10.1017/S0022112093003258.
- [22] Huete, C., Wouchuk, J. G., and Velikovich, A. L., "Analytical Linear Theory for the Interaction of a Planar Shock Wave with a Two- or Three-Dimensional Random Isotropic Acoustic Wave Field," *Physical Review E*, Vol. 85, 2012, p. 026312. https://doi.org/10.1103/PhysRevE.85.026312.
- [23] Hesselink, L., and Sturtevant, B., "Propagation of Weak Shocks through a Random Medium," *Journal of Fluid Mechanics*, Vol. 196, 1988, pp. 513–553. https://doi.org/10.1017/S0022112088002800.
- [24] Keller, J., and Merzkirch, W., "Interaction of a Normal Shock Wave with a Compressible Turbulent Flow," *Experiments in Fluids*, Vol. 8, 1990, pp. 241–248. https://doi.org/10.1007/BF00187225.
- [25] Barre, S., Alem, D., and Bonnet, J. P., "Experimental Study of a Normal Shock/Homogeneous Turbulence Interaction," *AIAA Journal*, Vol. 34, No. 5, 1996, pp. 968–974. https://doi.org/10.2514/3.13175.
- [26] Agui, J. H., Briassulis, G., and Andreopoulos, Y., "Studies of Interactions of a Propagating Shock Wave with Decaying Grid Turbulence: Velocity and Vorticity Fields," *Journal of Fluid Mechanics*, Vol. 524, 2005, pp. 143–195. https://doi.org/10.1017/S0022112004002514.
- [27] Mai, C. L. N., "Near-Region Modification of Total Pressure Fluctuations by a Normal Shock in Low-Density Hypersonic Wind Tunnel," Ph.D. thesis, Texas A&M University, Texas, USA, 2014.
- [28] Andreopoulos, Y., Agui, J. H., and Briassulis, G., "Shock Wave-Turbulence Interactions," *Annual Review of Fluid Mechanics*, Vol. 32, 2000, pp. 309–345. https://doi.org/10.1146/annurev.fluid.32.1.309.
- [29] Lee, S., Lele, S. K., and Moin, P., "Direct Numerical Simulation of Isotropic Turbulence Interacting with a Weak Shock Wave," *Journal of Fluid Mechanics*, Vol. 251, 1993, pp. 533–562. https://doi.org/10.1017/S0022112093003519.
- [30] Larsson, J., and Lele, S. K., "Direct Numerical Simulation of Canonical Shock/Turbulence Interaction," *Physics of Fluids*, Vol. 21, 2009, p. 126101. https://doi.org/10.1063/1.3275856.
- [31] Larsson, J., Bermejo-Moreno, I., and Lele, S. K., "Reynolds- and Mach-Number Effects in Canonical Shock-Turbulence Interaction," *Journal of Fluid Mechanics*, Vol. 717, 2013, pp. 293–321. https://doi.org/10.1017/jfm.2012.573.
- [32] Ryu, J., and Livescu, D., "Turbulence Structure behind the Shock in Canonical Shock-Vortical Turbulence Interaction," *Journal of Fluid Mechanics*, Vol. 756, 2014, pp. R1 1–13. https://doi.org/10.1017/jfm.2014.477.
- [33] Lee, S., Lele, S. K., and Moin, P., "Interaction of Isotropic Turbulence with Shock Waves: Effect of Shock Strength," *Journal of Fluid Mechanics*, Vol. 340, 1997, pp. 225–247. https://doi.org/10.1017/S0022112097005107.
- [34] Jamme, S., Cazalbou, J. B., Torres, F., and Chassaing, P., "Direct Numerical Simulation of the Interaction between a Shock Wave and Various Types of Isotropic Turbulence," *Flow, Turbulence and Combustion*, Vol. 68, 2002, pp. 227–268. https://doi.org/10.1023/A:1021197225166.
- [35] Grube, N. E., Taylor, E. M., and Martín, M. P., "Direct Numerical Simulation of Shock-wave/Isotropic Turbulence Interaction," AIAA Paper 2009-4165, 2009. https://doi.org/10.2514/6.2009-4165.
- [36] Donzis, D. A., "Shock Structure in Shock-Turbulence Interactions," *Physics of Fluids*, Vol. 24, 2012, p. 126101. https://doi.org/10.1063/1.4772064.
- [37] Grube, N. E., "Shock Wave-Turbulence Interactions," Ph.D. thesis, Princeton University, 2020.
- [38] Lee, S., Lele, S. K., and Moin, P., "Simulation of Spatially Evolving Turbulence and the Applicability of Taylor's Hypothesis in Compressible Flow," *Physics of Fluids A*, Vol. 4, No. 7, 1992, pp. 1521–1530. https://doi.org/10.1063/1.858425.
- [39] Prasad, C., Huang, J., Duan, L., and Gaitonde, D. V., "On the nature of freestream disturbances in a two-dimensional supersonic test section," AIAA 2021-0162, 2021. https://doi.org/10.2514/6.2021-0162.
- [40] Goparaju, H., Liu, Y., Duan, L., and Gaitonde, D. V., "Supersonic transition induced by numerical tunnel disturbances," AIAA 2022-1826, 2022. https://doi.org/10.2514/6.2022-1826.
- [41] Jiang, G., and Shu, C., "Efficient Implementation of Weighted ENO Schemes," *Journal of Computational Physics*, Vol. 126, No. 1, 1996, pp. 202–228. https://doi.org/10.1006/jcph.1996.0130.

- [42] Ducros, F., Ferrand, V., Nicoud, F., Weber, C., Darracq, D., Gacherieu, C., and Poinsot, T., "Large-eddy simulation of the shock/turbulence interaction," *Journal of Computational Physics*, Vol. 152, No. 2, 1999, pp. 517–549. https://doi.org/10.1006/jcph.1999.6238.
- [43] Pirozzoli, S., "Stabilized non-dissipative approximations of Euler equations in generalized curvilinear coordinates," *Journal of Computational Physics*, Vol. 230, No. 8, 2011, pp. 2997–3014. doi:10.1016/j.jcp.2011.01.001, URL http://dx.doi.org/10.1016/j.jcp.2011.01.001.
- [44] Williamson, J., "Low-Storage Runge-Kutta Schemes," *Journal of Computational Physics*, Vol. 35, No. 1, 1980, pp. 48–56. https://doi.org/10.1016/0021-9991(80)90033-9.
- [45] Duan, L., Choudhari, M. M., and Wu, M., "Numerical Study of Acoustic Radiation due to a Supersonic Turbulent Boundary Layer," *Journal of Fluid Mechanics*, Vol. 746, 2014, pp. 165–192. https://doi.org/10.1017/jfm.2014.116.
- [46] Duan, L., Choudhari, M. M., and Zhang, C., "Pressure Fluctuations Induced by a Hypersonic Turbulent Boundary Layer," *Journal of Fluid Mechanics*, Vol. 804, 2016, pp. 578–607. https://doi.org/10.1017/jfm.2016.548.
- [47] Liu, Y., Schuabb, M., Duan, L., Paredes, P., and Choudhari, M., "Interaction of a Tunnel-like Acoustic Disturbance Field with a Blunt Cone Boundary Layer at Mach 8," AIAA AVIATION Forum, 2022. To appear.
- [48] Xiong, Z., Nagarajan, S., and Lele, S. K., "Simple Method for Generating Inflow Turbulence," AIAA Journal, Vol. 42, No. 10, 2004, pp. 2164–2166. https://doi.org/10.2514/1.6157.
- [49] Larsson, J., "Blending Technique for Compressible Inflow Turbulence: Algorithm Localization and Accuracy Assessment," *Journal of Computational Physics*, Vol. 229, 2009, pp. 933–937. https://doi.org/10.1016/j.jcp.2008.10.027.
- [50] McKenzie, J. F., and Westphal, K. O., "Interaction of Linear Waves with Oblique Shock Waves," *Physics of Fluids*, Vol. 11, 1968, pp. 2350–2362. https://doi.org/10.1063/1.1691825.